Laser-assisted electron-argon scattering at small angles

Nathan Morrison and Chris H. Greene*

Department of Physics and JILA, University of Colorado, Boulder, Colorado 80309-0440, USA

(Received 10 September 2012; published 29 November 2012)

Electron-argon scattering in the presence of a linearly polarized, low-frequency laser field is studied theoretically. The scattering geometries of interest are small angles where momentum transfer is nearly perpendicular to the field, which is where the Kroll-Watson approximation has the potential to break down. The Floquet R matrix method solves the velocity gauge Schrödinger equation, using a larger reaction volume than previous treatments in order to carefully assess the importance of the long-range polarization potential to the cross section. A comparison of the cross sections calculated with the target potential fully included inside 20 and 100 a.u. shows no appreciable differences, which demonstrates that the long-range interaction cannot account for the high cross sections measured in experiments.

DOI: 10.1103/PhysRevA.86.053422 PACS number(s): 34.80.Qb

I. INTRODUCTION

Since the development of intense lasers, many studies have investigated the modification of familiar processes by the presence of coherent light. Particles that collide in the presence of a laser field can also exchange energy with the field in multiples of the laser frequency, a process known as laser-assisted collision. This paper investigates free-free transitions in electron scattering, where the state of the target atom remains unaltered.

In 1973 Kroll and Watson derived an expression for the cross section of a laser-assisted scattering event in terms of the elastic field-free cross section. Their main assumptions were that the time duration of the interaction is short compared to the laser cycle and that the target itself is unperturbed by the laser. They found the following expression [1]:

$$\frac{d\sigma_\nu}{d\Omega}(\mathbf{k}_f,\mathbf{k}_i) = \frac{k_f}{k_i} J_\nu^2(x) \frac{d\sigma_{\rm el}}{d\Omega}(\epsilon,\mathbf{Q}), \tag{1}$$

where ν denotes the number of laser photons absorbed by the electron ($-\nu$ is the number of photons emitted), $\mathbf{k}_f$ and $\mathbf{k}_i$ are the momenta of the final and initial electrons, J_ν is the Bessel function of the first kind of order ν, and $\frac{d\sigma_{\rm el}}{d\Omega}$ is the field-free elastic cross section. With the time-dependent laser vector potential of the form $\mathbf{A}(t) = \mathbf{A}_0 \sin(\omega t)$, the other parameters are defined as follows:

$$\mathbf{Q} = \mathbf{k}_f - \mathbf{k}_i, \tag{2}$$

$$x = -\frac{e\mathbf{A}_0 \cdot \mathbf{Q}}{mc\omega}, \tag{3}$$

$$\epsilon = \frac{k_i^2}{2m} - \nu\omega \frac{\hat{\mathbf{A}}_0 \cdot \mathbf{k}_i}{\hat{\mathbf{A}}_0 \cdot \mathbf{Q}} + \frac{m(\nu\omega)^2}{2(\hat{\mathbf{A}}_0 \cdot \mathbf{Q})^2}. \tag{4}$$

In addition to assuming that the laser frequency ω is small, the Kroll-Watson approximation (KWA) assumes that the dimensionless quantity x is sufficiently large that only on-shell scattering contributes.[1] This assumption becomes questionable not only when the parameters of the laser are changed but also in certain critical scattering geometries where $\mathbf{A}_0 \cdot \mathbf{Q} \approx 0$.

Wallbank and Holmes have performed experiments investigating these geometries for several neutral targets, beginning with helium and argon [2–4]. Their results show cross sections orders of magnitude greater than the Kroll-Watson prediction in regions where x is small. One of the first ideas proposed to explain this discrepancy was the polarization of the target by the field of the laser; however several separate theoretical treatments [5–7] showed such an effect to be negligible. It was also shown that for certain densities of the target gas, double scattering could account for the experimental signal [8]. Their determination of the experimental density was approximate, however, and to our knowledge the density dependence has not been confirmed experimentally.

Madsen and Taulbjerg [9] explore the derivation of the KWA, and they develop a generalized approximation by expanding the T matrix for weak fields and soft photons, but without assuming x is large. The region where the KWA loses its validity is therefore avoided. Their calculations show a few scattering geometries where the differential cross sections are comparable to the experimental cross sections. The shape of the experimental cross sections disagrees with the theory of Ref. [9], though, and there would have to be a very large uncertainty in the determination of the electron scattering angle for their calculations to explain the experimental cross sections at all angles.

The above treatments assume, as does the KWA, that only on-shell terms, i.e., terms where energy is conserved, contribute to the scattering event. A few later works use approximations that include off-shell contributions. Sun *et al.* [10] apply the second Born approximation. Jaroń and Kamiński [11,12] also use a similar off-shell approximation. They suggest that a diffraction effect due to a long-range potential, i.e., an interaction with a large extent compared to the electron deBroglie wavelength, could give rise to the sorts of cross sections at small angles seen in the experiment. The results of these in comparison with our calculations are discussed further in Sec. IV.

The advantage of R-matrix methods is that they provide an exact solution of the Schrödinger equation within the chosen reaction volume and so are limited only by the size of that volume and the numerical methods used in the calculation.

*Current address as of August 2012, Physics Department, Purdue University, West Lafayette, IN 47907.

[1] See Sec. 5 of Ref. [1].

Chen and Robicheaux [13] used a mixed-gauge R-matrix method with a reaction volume of 30 a.u. They calculated cross sections with an order of magnitude similar to that of the KWA.

The goal of this work is to use an exact R-matrix method with an expanded reaction volume. Including a longer range for the electron to interact with the induced dipole potential of the argon atom will clarify what contribution the long-range interaction has to the laser-assisted cross section. In Sec. II the details of the Floquet R-matrix method in the velocity gauge are laid out, and in Sec. III the connection to scattering states and the form of the scattering matrix are derived. Section IV discusses our numerical results, and Sec. V summarizes our findings. Atomic units are used throughout the rest of this paper.

II. FLOQUET R-MATRIX METHOD

The time and angle dependence of the electron wave function is represented by expanding in a product set of spherical harmonic and Floquet basis functions,

$$\Psi^{\beta}(\mathbf{r},t) = \sum_{\nu,l} \frac{F_{\nu l}^{\beta}(r)}{r} Y_{l0}(\Omega) \frac{e^{-i(E+\nu\omega)t}}{\sqrt{2\pi/\omega}}, \tag{5}$$

where β enumerates a complete set of linearly independent solutions of the Schrödinger equation. In order to make the treatment of larger reaction volumes tractable, this paper treats only scattering geometries where the incoming electron is parallel to the laser polarization. The cylindrical symmetry of this case allows setting $m_z = 0$ for the entire calculation, considerably reducing the number of basis functions needed.

Taking β as a column index, and combining the others into a row index, the radial functions can be thought of as composing a matrix $\underline{F}(r)$. With this the logarithmic derivative, or R matrix, is defined as

$$\underline{R}(r) = \underline{F}(r)[F'(r)^{-1}]. \tag{6}$$

The R matrix describes the behavior of the channel functions at the surface of a volume of constant radius r.

The R matrix is found by solving the Hamiltonian in the velocity gauge for an electron scattering off of a potential. The wavelength of the laser is around 2×10^5 a.u., which is much larger than the region of interaction of interest, so the vector potential is essentially constant in space. This leads to the following form for the Hamiltonian:

$$H = \frac{\mathbf{p}^2}{2} - \frac{1}{c}\mathbf{A}\cdot\mathbf{p} + V(r). \tag{7}$$

The target atom is represented by a model potential, borrowed from Chen and Robicheaux [13], containing a shielded Coulombic core and a long-range induced-dipole term:

$$V(r) = -\frac{Z}{r}e^{-a_1 r} - a_2 e^{-a_3 r} - \frac{\alpha}{2r^4}\left(1 - e^{-(r/r_{\rm cut})^3}\right)^2, \tag{8}$$

where $Z = 18$, the atomic number, and $\alpha = 10.77$, the argon polarizability. The other parameters of the model potential, which were fitted to the field-free phase shifts for argon, are $a_1 = 3.04$, $a_2 = 10.62$, $a_3 = 1.83$, and $r_{\rm cut} = 1.76$.

A. Variational principle for the R matrix

An extension of the eigenchannel R-matrix method, adapted for the Floquet formalism and for the velocity gauge, yields the solution to the Schrödinger equation. The solution is calculated numerically within a finite reaction volume Σ. It is helpful to begin with the Schrödinger equation for the velocity gauge Hamiltonian in integral form. (Note that, for notational brevity, we employ notation commonly used in differential geometry throughout this section. Function arguments and differentials are omitted from the integrands, but the integral is unambiguous as the domain of integration is denoted as a subscript on the integral sign.) The Schrödinger equation is

$$\int_{\Sigma,T} \Psi^* i\frac{\partial\Psi}{\partial t} = \int_{\Sigma,T} \Psi^* \left(-\frac{1}{2}\nabla^2\Psi - \frac{i}{c}\mathbf{A}\cdot\nabla\Psi + V(r)\Psi\right). \tag{9}$$

The full version of the energy operator is necessary due to the fact that, in the Floquet formalism, wave functions can be superpositions of states with different energies $E + \nu\omega$, which is the electron's kinetic energy at infinity. The only restriction on the space of wave functions considered is that the spatial inner product between any two wave functions is periodic, i.e.,

$$\int_{\Sigma} \Psi_1^* \Psi_2(t) = \int_{\Sigma} \Psi_1^* \Psi_2(t+T). \tag{10}$$

This is a reasonable assumption based on the fact that the Hamiltonian is itself periodic.

Application of the first Green identity to the kinetic term gives a term with the derivative on the surface $\partial\Sigma$:

$$\frac{1}{2}\int_{\partial\Sigma,T} \Psi^*\frac{\partial\Psi}{\partial n} = \int_{\Sigma,T}\left(\frac{1}{2}\nabla\Psi^*\cdot\nabla\Psi - \frac{i}{c}\mathbf{A}\cdot\Psi^*\nabla\Psi + V(r)\Psi^*\Psi - \Psi^* i\frac{\partial\Psi}{\partial t}\right). \tag{11}$$

This is the usual starting point to find a variational principle for the logarithmic derivative. Because the velocity gauge contains a first derivative term, however, this must be taken into account in order to construct a variational principle. Using a form of the divergence theorem, the identity becomes

$$\begin{aligned}\frac{1}{2}\int_{\partial\Sigma,T}\left(\Psi^*\frac{\partial\Psi}{\partial n} + \frac{i}{c}\mathbf{A}\cdot\hat{\mathbf{n}}\Psi^*\Psi\right) &= \int_{\Sigma,T}\left(\frac{1}{2}\nabla\Psi^*\cdot\nabla\Psi - \frac{i}{2c}\mathbf{A}\cdot(\Psi^*\nabla\Psi - \nabla\Psi^*\Psi)\right.\\ &\left. + V(r)\Psi^*\Psi - \Psi^* i\frac{\partial\Psi}{\partial t}\right).\end{aligned} \tag{12}$$

Now define the operator $\tilde{L}$ as follows:

$$\tilde{L}\Psi = \frac{\partial\Psi}{\partial n} + \frac{i}{c}\mathbf{A}\cdot\hat{\mathbf{n}}\Psi. \tag{13}$$

The set of channel functions in all surface coordinates forms a linear space on the surface of Σ. Consider wave functions Ψ_β that are eigenfunctions of $\tilde{L}$ on this surface, i.e., $\tilde{L}\Psi_\beta|_{\partial\Sigma} = b_\beta\Psi_\beta|_{\partial\Sigma}$. The value b_β corresponds to the term of the same name used by Aymar *et al.* [14], except for being defined with the opposite sign. It is the usual logarithmic derivative with

one term added:

$$b_\beta = \left(\frac{1}{\Psi_\beta}\frac{\partial \Psi_\beta}{\partial n} + \frac{i}{c}\mathbf{A}\cdot\hat{\mathbf{n}}\right)_{\partial\Sigma} = \left(\frac{\partial \ln(\Psi_\beta)}{\partial n} + \frac{i}{c}\mathbf{A}\cdot\hat{\mathbf{n}}\right)_{\partial\Sigma}. \tag{14}$$

The following functional is the variational principle for the eigenvalues b_β of the generalized logarithmic derivative operator:

$$b[\Psi] = 2\frac{\int_{\Sigma,T}\left(\frac{1}{2}\nabla\Psi^*\cdot\nabla\Psi - \frac{i}{2c}\mathbf{A}\cdot(\Psi^*\nabla\Psi - \nabla\Psi^*\Psi) + V(r)\Psi^*\Psi - \Psi^* i\frac{\partial\Psi}{\partial t}\right)}{\int_{\partial\Sigma,T}\Psi^*\Psi}. \tag{15}$$

It can be shown that the first variation $\delta b[\Psi_\beta]$ vanishes for all deviations $\delta\Psi$ from the exact solution. To show this, integrate by parts and use the periodicity restriction (10) on the energy operator:

$$\delta\left(\int_{\Sigma,T}\Psi^* i\frac{\partial\Psi}{\partial t}\right) = \int_{\Sigma,T}\delta\Psi^* i\frac{\partial\Psi}{\partial t} - \int_{\Sigma,T} i\frac{\partial\Psi^*}{\partial t}\delta\Psi. \tag{16}$$

Using this, the variation can be written

$$\begin{aligned}\delta b[\Psi_\beta] \propto \int_{\partial\Sigma,T}\Psi_\beta^*\Psi_\beta \int_{\Sigma,T}\left(\frac{1}{2}\nabla\delta\Psi_\beta^*\cdot\nabla\Psi_\beta - \frac{i}{2c}\mathbf{A}\cdot(\delta\Psi_\beta^*\nabla\Psi_\beta - \nabla\delta\Psi_\beta^*\Psi_\beta) + V(r)\delta\Psi_\beta^*\Psi_\beta - \delta\Psi_\beta^* i\frac{\partial\Psi_\beta}{\partial t}\right)\\ - \int_{\Sigma,T}\left(\frac{1}{2}\nabla\Psi_\beta^*\cdot\nabla\Psi_\beta - \frac{i}{2c}\mathbf{A}\cdot(\Psi_\beta^*\nabla\Psi_\beta - \nabla\Psi_\beta^*\Psi_\beta) + V(r)\Psi_\beta^*\Psi_\beta - \Psi_\beta^* i\frac{\partial\Psi_\beta}{\partial t}\right)\int_{\partial\Sigma,T}\delta\Psi_\beta^*\Psi_\beta + \text{c.c.}\end{aligned} \tag{17}$$

The first Green identity can now be applied to each of the kinetic terms, and the divergence theorem can be applied to the vector potential terms, to show the variation vanishes.

B. Solving for the *R* matrix

In practice we restrict ourselves to a spherical reaction volume S with radius r_0, centered on the origin, rather than the general reaction volume Σ. In this case the unit normal vector $\hat{\mathbf{n}}$ is the same as the unit radial vector $\hat{\mathbf{r}}$ on the surface ∂S. The numerical solution of the R matrix is carried out by expanding the wave function in a basis set: $\Psi = \sum_{pi} c_{pi}\psi_{pi}(\mathbf{r},t) = \sum_{pi} c_{pi}\frac{u_p(r)}{r}\Phi_i(\Omega,t)$, The radial basis functions $u_p(r)$ can in principle be arbitrary. In this calculation we have chosen radial basis functions according to a finite-element discrete-variable representation (FEM-DVR) of the kind described in Ref. [15]. The channel functions $\Phi_i(\Omega,t)$ have the form $\Phi_i = Y_{l_i0}(\Omega)\frac{e^{-i(E+v_i\omega)t}}{\sqrt{2\pi/\omega}}$. The variational principle (15) is then written as an eigenvalue equation, $\underline{\Lambda}\,\underline{c}\,b = \underline{\Gamma}\,\underline{c}$, with the following definitions for the matrices:

$$\Gamma_{pi,qj} = \int_{S,T}\psi_{pi}^*\left(H - i\frac{\partial}{\partial t}\right)\psi_{qj} + \int_{\partial S,T}\psi_{pi}^* L\psi_{qj}, \tag{18}$$

$$\Lambda_{pi,qj} = \int_{\partial S,T}\psi_{pi}^*\psi_{qj}. \tag{19}$$

Here L is the usual Bloch operator with the field term, defined so that $L\Psi = \frac{1}{r}\frac{\partial r\Psi}{\partial r} + \frac{i}{c}\mathbf{A}\cdot\hat{\mathbf{n}}\Psi$, whose eigenvalues are the logarithmic derivative of the reduced wave function. This differs from $\tilde{L}$ in Eq. (13) only by the addition of one Hermitian term, so it is still variational. Only a small subset of the basis functions have nonzero value on the surface of the reaction volume, which allows the full eigenvalue equation to be reduced using the method of Greene and Kim [16]. Denoting these open type basis functions with o and the others with c, the eigenvalue equation can be written as follows:

$$\begin{pmatrix}0 & 0\\ 0 & \underline{\Lambda}_{oo}\end{pmatrix}\begin{pmatrix}\underline{c}_c\\ \underline{c}_o\end{pmatrix}b = \begin{pmatrix}\underline{\Gamma}_{cc} & \underline{\Gamma}_{co}\\ \underline{\Gamma}_{oc} & \underline{\Gamma}_{oo}\end{pmatrix}\begin{pmatrix}\underline{c}_c\\ \underline{c}_o\end{pmatrix}. \tag{20}$$

The eigenvalue equation can then be rearranged as follows:

$$\underline{\Lambda}_{oo}\underline{c}_o b = \underline{\Omega}\,\underline{c}_o, \quad \underline{\Omega} = \underline{\Gamma}_{oo} - \underline{\Gamma}_{oc}\underline{\Gamma}_{cc}^{-1}\underline{\Gamma}_{co}, \tag{21}$$

which places most of the load of the calculation on the linear solution for $\underline{\Gamma}_{cc}^{-1}\underline{\Gamma}_{co}$, which requires fewer resources than a full diagonalization, although it must be solved for each collision energy of interest. The matrix R is then calculated from the eigenvalues and eigenvectors found from Eq. (21). The resulting R matrix is symmetric and is related to the reduced wave function $\underline{F}(r)$ as follows:

$$\underline{R}^{-1}(r) = \underline{F}'(r)[F(r)]^{-1} + \underline{W}, \tag{22}$$

$$W_{i,j} = \frac{i}{c}\int_0^T dt \oint d\Omega\, \Phi_i^*(\Omega,t)\mathbf{A}(t)\cdot\hat{\mathbf{n}}(\Omega)\Phi_j(\Omega,t). \tag{23}$$

III. SCATTERING IN A LASER FIELD

A. Matching to scattering solutions

The vector potential term in the Schrödinger equation can be removed by the following transformation [17]:

$$\Phi = \Omega\Psi, \quad \Omega = \exp\left(\frac{i}{c}\int^t \mathbf{A}(\tau)\cdot\mathbf{p}\,d\tau\right). \tag{24}$$

After defining $\boldsymbol{\alpha}(t) = \frac{1}{c}\int^t \mathbf{A}(\tau)\,d\tau$, it becomes clear that Ω is a translation operator; i.e., for functions of position, $\Omega f(\mathbf{r}) = f[\mathbf{r}+\boldsymbol{\alpha}(t)]\Omega$. It follows simply that Φ obeys the equation

$$i\frac{\partial\Phi}{\partial t} = -\frac{1}{2}\nabla^2\Phi + V(|\mathbf{r}+\boldsymbol{\alpha}(t)|), \tag{25}$$

which at large r approaches the free space Hamiltonian, because $V(r)\to 0$ faster than $\frac{1}{r}$. We may therefore match

to free space scattering solutions of the form

$$\Phi^{\beta} = \sum_i Y_{l_i 0}(\theta,\phi)\frac{e^{-i(E+\nu_i\omega)t}}{\sqrt{2\pi/\omega}}\frac{f_i\delta_i^{\beta} - g_i K_i^{\beta}}{r}, \tag{26}$$

where $\underline{K}$ is the short-range reaction matrix and the scattering states are

$$f_i = \sqrt{\frac{2k_i}{\pi}} r\, j_{l_i}(k_i r) \quad \text{and} \quad g_i = \sqrt{\frac{2k_i}{\pi}} r\, n_{l_i}(k_i r). \tag{27}$$

The electron energy in each channel i, as it relates to the floquet index ν_i and the wave number k_i, is $\epsilon_i = E + \nu_i\omega = \frac{1}{2}k_i^2$. Using the reverse translation, $\Psi = \Omega^{-1}\Phi$, and defining functions $\rho(t)$ and $\theta(t)$ that describe the length and angle of $\boldsymbol{\rho}(t) = \mathbf{r} - \boldsymbol{\alpha}(t)$, the velocity gauge wave function can be written as

$$\Psi^{\beta} = \sum_i Y_{l_i 0}[\theta(t),\phi]\frac{e^{-i(E+\nu_i\omega)t}}{\sqrt{2\pi/\omega}}\frac{f_i[\rho(t)] - g_i[\rho(t)]K_i^{\beta}}{\rho(t)}. \tag{28}$$

Following Varró and Ehlotzky [18], this can be projected onto the original basis set in the untranslated coordinates, resulting in

$$\Psi^{\mu\lambda}(\mathbf{r},t) = \sum_{\nu l,\xi j}\Phi_{\nu l}(\Omega,t)\frac{\mathfrak{f}_{\nu l}^{\xi j}(r)\delta_{\xi}^{\mu}\delta_j^{\lambda} - \mathfrak{g}_{\nu l}^{\xi j}(r)K_{\xi j}^{\mu\lambda}}{r}, \tag{29}$$

$$\mathfrak{f}_{\nu l}^{\xi j}(r) = \sqrt{\frac{2k_{\xi}}{\pi}} B_{l,\nu-\xi}^{\xi j}\, r j_l(k_{\xi} r), \tag{30}$$

$$\mathfrak{g}_{\nu l}^{\xi j}(r) = \sqrt{\frac{2k_{\xi}}{\pi}} B_{l,\nu-\xi}^{\xi j}\, r n_l(k_{\xi} r), \tag{31}$$

$$B_{ls}^{\xi j} = \frac{i^{j-l-s}}{2}\sqrt{(2j+1)(2l+1)} \times \int_{-1}^{1} dx\, P_j(x)P_l(x)J_s(-k_{\xi}\alpha_0 x), \tag{32}$$

where in Eq. (32), α_0 refers to the amplitude of the jitter motion $\boldsymbol{\alpha}(t)$, i.e., for our particular choice of coordinates and time $\boldsymbol{\alpha}(t) = \alpha_0\cos(\omega t)\hat{\mathbf{z}}$.

Identifying channel indices (ν,l) as row indices, and indices for linearly independent solutions (μ,λ) as column indices, Eq. (29) can be summarized in matrix form for the reduced wave function as in Eq. (5):

$$\underline{F}(r) = \underline{\mathfrak{f}}(r) - \underline{\mathfrak{g}}(r)\underline{K}, \tag{33}$$

and using Eq. (22), $\underline{K}$ can be found in terms of $\underline{R}$:

$$\underline{K} = \{[\underline{R}^{-1}(r_0) - \underline{W}]\underline{\mathfrak{g}}(r_0) - \underline{\mathfrak{g}}'(r_0)\}^{-1} \times \{[\underline{R}^{-1}(r_0) - \underline{W}]\underline{\mathfrak{f}}(r_0) - \underline{\mathfrak{f}}'(r_0)\}. \tag{34}$$

Note that although $\underline{W}$, $\underline{\mathfrak{f}}$, and $\underline{\mathfrak{g}}$ are not symmetric, this approach yields a reaction matrix that is symmetric and real.

B. Calculating the cross section

The asymptotic form of the wave function in this Floquet picture is

$$\Psi(\mathbf{r},t) = e^{i(k_0 z - Et)} + \sum_{\nu\in Z} f_{\nu}(\theta)\frac{e^{i[k_{\nu}r-(E+\nu\omega)t]}}{r}, \tag{35}$$

and the cross section for each Floquet channel follows from this:

$$\frac{d\sigma_{\nu}}{d\Omega} = \frac{r^2|\hat{\mathbf{r}}\cdot\mathbf{j}_{\text{out},\nu}|}{|\mathbf{j}_{\text{inc}}|} = \frac{k_{\nu}}{k_0}|f_{\nu}(\theta)|^2. \tag{36}$$

This can be expressed in terms of the scattering matrix $\underline{S} = (\underline{1} + i\underline{K})(\underline{1} - i\underline{K})^{-1}$:

$$\frac{d\sigma_{\nu}}{d\Omega} = \frac{1}{k_0^2}\left|\sum_{l,l'=0}^{\infty}\sqrt{\pi(2l'+1)} \times (i^{l'-l}S_{\nu l,0l'} - \delta_{l,l'}\delta_{\nu,0})Y_{l,0}(\theta,0)\right|^2, \tag{37}$$

where the phase factor $i^{l'-l}$ above is a result of the choice of phase in the scattering functions (27).

IV. RESULTS

Figure 1 contains our calculation of the cross section along with a comparison calculation using the KWA. The collision

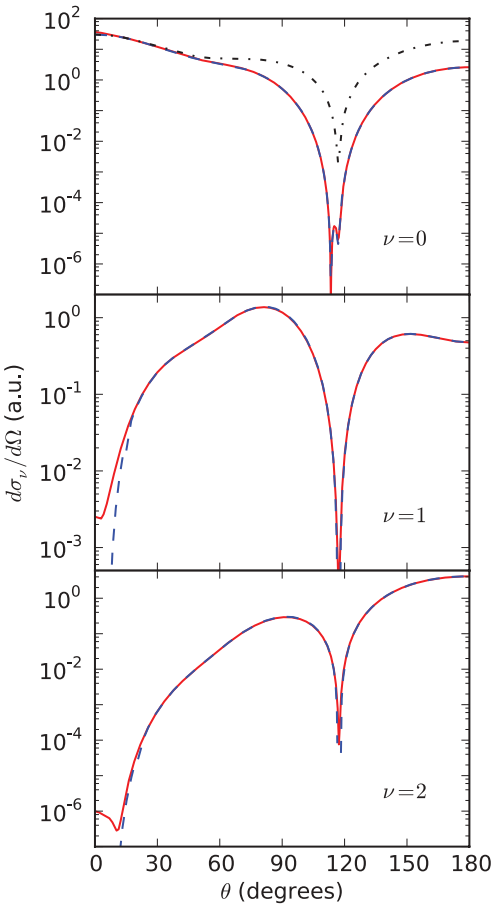

FIG. 1. (Color online) Differential cross section for electrons absorbing zero (top) to two (bottom) photons. The solid red line is the cross section found with the Floquet R-matrix calculation, and the dashed blue line is calculated using the KWA. This calculation was performed with the R-matrix boundary at 100 a.u., with 19 total Floquet channels and angular momentum channels up to $l = 150$. The theoretical field-free cross section is included in the top box for comparison, in black with dashes and dots.

parameters were chosen to mimic the experiment: a laser intensity of 5×10^7 W cm^{-2}, which corresponds to a jitter motion amplitude $\alpha_0 = 2.0$ a.u., a photon energy of 0.12 eV, and an electron energy of 10 eV. It is worth noting that the electron energy lies below the first excitation channel of argon, so it makes sense to keep just the single channel for the target. The boundary of the reaction volume for this calculation is at $r_0 = 100$ a.u. Note that this is much larger than α_0.

The calculation shown in Fig. 1 contains 19 Floquet channels up to $\nu = \pm 9$ and angular momentum channels up to $l = 150$ for a total of 2869 channels on the surface of the volume. This is the size of one dimension of the matrices $\underline{R}$, $\underline{K}$, etc. This number of angular momenta is needed to converge the matching equations for the scattering solution; as is shown in Eq. (30), the regular scattering solutions are proportional to $j_l(kr_0)$, which has significant value when $l \approx kr_0$. The number of Floquet channels needed for convergence increases with r_0 as well, but this has more to do with the numerical convergence of the R matrix solution than with the matching. The field is constant in space, so a larger reaction volume means more matrix elements coupling the Floquet channels. For the FEM-DVR radial basis, several different combinations of sector spacing and DVR order were calculated and compared to one another to assess convergence. The presented calculation uses three DVR sectors spaced such that sectors closer to the origin, where the electron's de Broglie wavelength is shorter, have a shorter extent. Each sector contains grid points spaced according to a Gauss-Lobatto quadrature with 75 nodes. We found that, in most instances, increasing the order of the quadrature yields faster convergence relative to computation time than increasing the number of sectors, despite the fact that the latter yields sparser matrices. The total number of radial basis functions is 222, and the total number of basis functions represented in the linear solution step of Eq. (21) is the product of this and the number of channels, over 600 000. These matrices are quite sparse, and the linear solution is carried out with PARDISO. For Floquet channels $\nu = 1$ and $\nu = 2$, the differential cross sections are converged with respect to basis size to within 10^{-2} and 10^{-3} a.u. in absolute units of the maximum difference between calculations and to within 1% of the cross section value at all angles.

Note that the Floquet R-calculation and the KWA agree very well for all but very small scattering angles. Also included in the top plot is the elastic field-free cross section for this model potential, which essentially results from a fit [13] to the experimental phase shifts found by Furst *et al.* [19]. Note that the the angle of the cross-section minimum corresponds to the field-free minimum and that the value of the field-free differential cross section and that for $\nu = 0$ agree at zero angle. The Floquet differential cross sections also sum to a value that is indistinguishable from the field-free cross section, but this is not depicted.

Figure 2 shows the differential cross section at 9° for absorption and emission of up to four photons, again compared with the KWA result. Note that though the results do not agree exactly, they differ by far fewer orders of magnitude than those measured by Wallbank and Holmes at this scattering angle. For example, the differential cross sections they found for exchanges of one and two photons were on the order of 1% of the field-free elastic differential cross section, while

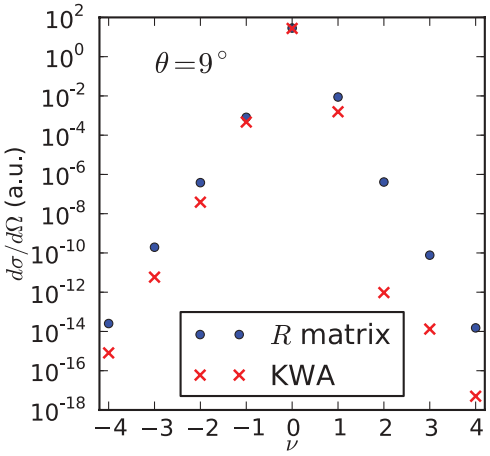

FIG. 2. (Color online) Differential cross sections at 9° versus the number ν of photon energies gained by the electron. The cross section found via the R-matrix calculation (blue dots) has comparable order of magnitude to the KWA (red crosses) for a few photon numbers, and it is several orders of magnitude smaller than the experimental results for all nonzero ν. The parameters of the calculation are the same as those for Fig. 1.

our calulations show these as roughly 10^{-2}% and 10^{-6}%, respectively.

Differential cross sections calculated with R-matrix boundaries from 10 to 100 a.u. show no differences that are distinguishable from the convergence with respect to the basis. Our differential cross section also agrees with that of Chen and Robicheaux [13], who used a variable gauge approach and chose an R-matrix boundary of 30 a.u. We can, therefore, rule out the possibility that the long-range induced-dipole potential would yield the sort of diffraction suggested by Jaroń and Kamiński [12] over distances comparable to or even several times the electron de Broglie wavelength.

It has been suggested that uncertainty in the scattering angle could account for higher observed cross sections. Madsen and Taulbjerg [9] even suggest that the incoming electron beam is poorly collimated, leading to an effective error in the scattering angle as high as 8°, as opposed to the 2° reported from the detector width [4]. Convolving the cross sections shown in Fig. 1 with a Gaussian having a width up to 8° does not give a significant difference in the one- and two-photon cross sections, however. Whatever the source of such an error, uncertanties in the scattering angle would not explain the experimental cross sections for this geometry.

Sun *et al.* [10] calculate a cross section for a one-photon exchange that is quantitatively quite close to our result. Their result for a two-photon exchange is several orders of magnitude higher, however. This may be due to a convergence issue, as a group using a similar method for laser-assisted helium scattering at first found high cross sections [11], but later found better results that are closer to the KWA [20].

V. CONCLUSIONS

The Floquet R-matrix method provides an exact solution of the Schrödinger equation in the velocity gauge. By comparing cross sections calculated with R-matrix boundaries up to

100 a.u., over ten times the de Broglie wavelength of a 10-eV electron, we have shown that the induced dipole potential for argon does not contribute to the laser-assisted cross section. This is true even at small angles where the momentum transfer has a very small component along the field, and so the KWA is less valid. Diffraction from this long-range piece of the potential cannot account for the high cross sections found in the experiments of Wallbank and Holmes [2–4], which are several orders of magnitude higher than both the approximation and our calculations.

The most plausible explanation for the experimental results remains multiple scattering. Later experiments for helium by the same group claim to see the same high cross sections even when the gas is too dilute for multiple scattering to play a significant role [21], so it is unclear whether this is the correct explanation. To our knowledge, a similar experiment for argon including characterization of the gas density has not been performed.

ACKNOWLEDGMENTS

Discussions with A. Jaron-Becker and M. Tarana are much appreciated. We gratefully acknowledge the support of the Department of Energy, Office of Science.

[1] N. M. Kroll and K. M. Watson, Phys. Rev. A **8**, 804 (1973).
[2] B. Wallbank and J. K. Holmes, Phys. Rev. A **48**, R2515 (1993).
[3] B. Wallbank and J. K. Holmes, J. Phys. B **27**, 1221 (1994).
[4] B. Wallbank and J. K. Holmes, J. Phys. B **27**, 5405 (1994).
[5] I. Rabadán, L. Méndez, and A. S. Dickinson, J. Phys. B **27**, L535 (1994).
[6] S. Geltman, Phys. Rev. A **51**, R34 (1995).
[7] S. Varró and F. Ehlotzky, Phys. Lett. **203**, 203 (1995).
[8] I. Rabadán, L. Méndez, and A. S. Dickinson, J. Phys. B **29**, L801 (1996).
[9] L. B. Madsen and K. Taulbjerg, J. Phys. B **28**, 5327 (1995).
[10] J. Sun, S. Zhang, Y. Jiang, and G. Yu, Phys. Rev. A **58**, 2225 (1998).
[11] A. Jaroń and J. Z. Kamiński, Phys. Rev. A **56**, R4393 (1997).
[12] A. Jaroń and J. Z. Kamiński, Laser Phys. **9**, 81 (1999).
[13] C.-T. Chen and F. Robicheaux, J. Phys. B **29**, 345 (1996).
[14] M. Aymar, C. H. Greene, and E. Luc-Koenig, Rev. Mod. Phys. **68**, 1015 (1996).
[15] O. I. Tolstikhin, S. Watanabe, and M. Matsuzawa, J. Phys. B **29**, L389 (1996).
[16] C. H. Greene and L. Kim, Phys. Rev. A **38**, 5953 (1988).
[17] W. C. Henneberger, Phys. Rev. Lett. **21**, 838 (1968).
[18] S. Varró and F. Ehlotzky, Z. Phys. D **8**, 211 (1988).
[19] J. E. Furst, D. E. Golden, M. Mahgerefteh, J. Zhou, and D. Mueller, Phys. Rev. A **40**, 5592 (1989).
[20] L. W. Garland, A. Jaron, J. Z. Kaminski, and R. M. Potvliege, J. Phys. B **35**, 2861 (2002).
[21] B. Wallbank and J. K. Holmes, Can. J. Phys. **79**, 1237 (2001).